Molecular Pharmacology Fast Forward. Published on September 9, 2021 as DOI: 10.1124/molpharm.121.000357
This article has not been copyedited and formatted. The final version may differ from this version.

Construction and characterization of CRISPR/Cas9 knockout rat model of carboxylesterase 2a gene

Jie Liu[a,#], Xuyang Shang[a,#], Shengbo Huang[a], Yuan Xu[a], Jian Lu[a], Yuanjin Zhang[a], Zongjun Liu[b,*], Xin Wang[a,*]

[a]Shanghai Key Laboratory of Regulatory Biology, Institute of Biomedical Sciences and School of Life Sciences, East China Normal University, Shanghai 200241, China

[b]Department of Cardiology, Central Hospital of Shanghai Putuo District, Shanghai University of Traditional Chinese Medicine, Shanghai 200062, China.

[#]These authors contributed equally to this work.

Molecular Pharmacology Fast Forward. Published on September 9, 2021 as DOI: 10.1124/molpharm.121.000357
This article has not been copyedited and formatted. The final version may differ from this version.

Running Title: CRISPR Knockout Rat Ces2a Model

Address correspondence to:

Dr. Xin Wang,

School of Life Sciences, East China Normal University, Shanghai 200241, China.

E-mail address: xwang@bio.ecnu.edu.cn

Dr. Zongjun Liu

Central Hospital of Shanghai Putuo District, Shanghai University of Traditional Chinese Medicine, Shanghai 200062, China.

E-mail address: lzj72@126.com

Number of text pages:36

Number of tables: 4

Number of figures: 7

Number of references: 43

Number of words in the Abstract:193

Number of words in the Introduction:600

Number of words in the Materials and Methods:1867

Number of words in the Results:1215

Number of words in the Discussion:1246

List of abbreviations:

ALB, albumin; ALB/GLB, albumin/globulin ratio; ALP, alkaline phosphatase; ALT, alanine aminotransferase; AST, aspartate aminotransferase; AST/ALT, aspartate aminotransferase/alanine aminotransferase; AUC, area under the drug

Molecular Pharmacology Fast Forward. Published on September 9, 2021 as DOI: 10.1124/molpharm.121.000357
This article has not been copyedited and formatted. The final version may differ from this version.

concentration-time curve; CAR, constitutive active/androstane receptor; CES, carboxylesterase; CI, confidence interval; C_{Lint}, intrinsic clearance; CL, clearance; C_{max}, maximum concentration; CRISPR-Cas9, clustered regularly interspaced short palindromic repeats-CRISPR-associated protein-9 nuclease; DBL, direct bilirubin; DDI, drug-drug interactions; GLB, globulin; GLU, glucose; GTT, glucose tolerance test; HDL-C, high density lipoprotein cholesterol; H&E, Haemotoxylin and Eosin; HNF4α, hepatocyte nuclear factor 4alpha; IBIL, indirect bilirubin; ITT, insulin tolerance test; K_m, michaelis constant; LDL-C, low density lipoprotein cholesterol; MRT, mean residence time; NAFLD, non-alcoholic fatty liver disease; PAM, protospacer adjacent motif; PPARα, peroxisome proliferator-activated receptors-alpha; PXR, pregnane X receptor; RLM, rat liver microsomes; SD, Sprague-Dawley; sgRNA, single guide RNA; TBA, total bile acid; TBL, total bilirubin; T-CH, total cholesterol; TG, triglyceride; T_{max}, peak time; TP, total protein.

Molecular Pharmacology Fast Forward. Published on September 9, 2021 as DOI: 10.1124/molpharm.121.000357
This article has not been copyedited and formatted. The final version may differ from this version.

Abstract

Carboxylesterase 2 (CES2), an important metabolic enzyme, plays a critical role in drug biotransformation and lipid metabolism. Although CES2 is very important, few animal models have been generated to study its properties and functions. Rat *Ces2* is similar to human *CES2A-CES3A-CES4A* gene cluster, with highly similar gene structure, function and substrate. In this report, CRISPR/Cas9 technology was firstly used to knock out rat *Ces2a*, a main subtype of *Ces2* mostly distributed in liver and intestine. This model showed the absence of CES2A protein expression in liver. Further pharmacokinetic studies of diltiazem, a typical substrate of CES2A, confirmed the loss of function of CES2A both *in vivo* and *in vitro*. At the same time, the expression of CES2C and CES2J protein in liver decreased significantly. The body and liver weight of *Ces2a* knockout rats also increased, but the food intake did not change. Moreover, the deficiency of *Ces2a* led to obesity, insulin resistance and liver fat accumulation, which are consistent with the symptoms of nonalcoholic fatty liver disease (NAFLD). Therefore, this rat model is not only a powerful tool to study drug metabolism mediated by CES2, but also a good disease model to study NAFLD.

Keywords: Carboxylesterase 2; CRISPR/Cas9; Lipid metabolism; NAFLD; Rat model

Molecular Pharmacology Fast Forward. Published on September 9, 2021 as DOI: 10.1124/molpharm.121.000357
This article has not been copyedited and formatted. The final version may differ from this version.

Significance statement：

Human CES2 plays a key role in the first-pass hydrolysis metabolism of most oral prodrugs as well as lipid metabolism. In this study, CRISPR/Cas9 technology was used to knock out Ces2a gene in rats for the first time. This model can be used not only in the study of drug metabolism and pharmacokinetics, but also as a disease model of NAFLD and other metabolic disorder.

Molecular Pharmacology Fast Forward. Published on September 9, 2021 as DOI: 10.1124/molpharm.121.000357
This article has not been copyedited and formatted. The final version may differ from this version.

Introduction

Carboxylesterase (CES), a kind of α/β serine folding protein, is one of the most important phase I drug metabolizing enzymes, belonging to the class B esterase (IMAI, 2006; Oda et al., 2015). Human CES superfamily is divided into five families (CES1, CES2, CES3, CES4A, CES5A), among which CES1 may exist in the form of monomer, trimer or hexamer, while CES2 and CES3 mostly exist in the form of monomer (Fleming et al., 2007; Holmes et al., 2010; Kim et al., 1997). CES1 and CES2, as the main subtypes of carboxylesterase, have 47% amino acid sequence similarity. However, they have a clear tendency in the choice of substrates (Satoh and Hosokawa, 2006). CES1 tends to hydrolyze ester bonds with larger acyl moieties and smaller alcohol moieties, while CES2 prefers to select ester bond compounds with smaller acyl moieties and relatively large alcohol moieties as substrates (Di, 2019). CES2 is distributed widely in the small intestine, liver, colon and kidney (Boberg et al., 2017; Sato et al., 2012). As one of the most abundant carboxylesterase subtypes in the gastrointestinal tract, CES2 mediates the first-pass hydrolysis metabolism of most oral prodrugs (Laizure et al., 2013), including a variety of clinical drugs, such as anticancer drugs: capecitabine and flutamide (Abdelwahab et al., 2018; Xu et al., 2002), angiotensin receptor antagonist: candesartan and olmesartan (Nishikawa et al., 1997; Ma et al., 2005), as well as many drugs affecting the central nerve system (CNS) such as heroin and cocaine (Kamendulis et al., 1996). Since the liver is the center of metabolism in the body of most drugs, especially drugs containing ester bonds, the

Molecular Pharmacology Fast Forward. Published on September 9, 2021 as DOI: 10.1124/molpharm.121.000357
This article has not been copyedited and formatted. The final version may differ from this version.

total clearance of these drugs mainly depends on CES2. Inhibition of CES2 activity can lead to changes of drug exposure and result in serious side effects. With the emergence of clinical drugs containing ester bonds, more drug-drug interactions (DDI) based on CES2 need to be further explored.

Human CES2 also plays an indispensable role in lipid metabolism. Lipid homeostasis regulated by CES2 is achieved through lipid hydrolysis, fatty acid oxidation, endoplasmic reticulum stress and lipid synthesis (Lian et al., 2018). Previous studies have shown that the expression of CES2 in the liver of patients with nonalcoholic fatty liver disease (NAFLD) is significantly decreased, and the activity of CES2 is also decreased in obese patients (Li et al., 2016). However, transferring human CES2 into mice can significantly improve the disorder of liver lipid metabolism (Ruby et al., 2017). In addition, the expression of CES2 is directly or indirectly controlled by the activation of transcription factors, such as pregnane X receptor (PXR), constitutive active/androstane receptor (CAR), peroxisome proliferator-activated receptors-alpha (PPARα), hepatocyte nuclear factor 4alpha (HNF4α). These transcription factors are also closely related to the occurrence and development of NAFLD (Furihata et al., 2006; Staudinger et al., 2010), but the regulation of CES2 still needs further study. Therefore, it is urgent to establish reliable and practical animal models to study the role of CES2 in pathology and clinical medicine.

Molecular Pharmacology Fast Forward. Published on September 9, 2021 as DOI: 10.1124/molpharm.121.000357
This article has not been copyedited and formatted. The final version may differ from this version.

Rat *Ces2a* is the main subtype of *Ces2*, and its gene structure, function and substrate are highly similar with humans. Clustered regularly interspaced short palindromic repeats/CRISPR-associated protein-9 nuclease (CRISPR/Cas9) technology, as the third-generation artificial nuclease technology, has become a powerful gene editing tool. Due to its practicability, simplicity and high efficiency (Torres-Ruiz and Rodriguez-Perales, 2017), it is engineered for genome editing and then applied to the establishment of animal models, which greatly speeds up the pace of research (Hryhorowicz et al., 2017).

In this study, the *Ces2a* gene was knocked out in rats by CRISPR/Cas9 technology for the first time, and the *Ces2a* knockout (KO) rat model was successfully constructed and characterized. This model can be used not only in drug metabolism and pharmacokinetics, but also as a disease model of metabolic disorder, such as NAFLD.

Materials and method

Reagents

Oligos (60 bp, containing *Ces2a* KO target sites) and all primers for PCR/Q-PCR were synthesized by Biosune Biotechnology Co., Ltd (Shanghai, China). SYBR Green real-time fluorescence quantitative PCR master mix and Reverse transcription kit was purchased from Yeasen (Shanghai, China). T7 *in vitro* transcription kit and RNAiso Plus were bought from TaKaRa (Dalian, China). Bicinchoninic acid kit and

Molecular Pharmacology Fast Forward. Published on September 9, 2021 as DOI: 10.1124/molpharm.121.000357
This article has not been copyedited and formatted. The final version may differ from this version.

SP6 *in vitro* transcription kit were obtained from Thermo Scientific (Waltham, MA, USA). Blood glucose meter was from Johnson (New Brunswick, NJ, USA). D-Glucose, insulin-human and diltiazem were obtained from Meilun Biotech Co. Ltd (Dalian, China). Deacetyldiltiazem was bought from Toronto Research Chemicals Inc. (Ontario, NY, Canada).

Animals

Male and female Sprague-Dawley (SD) rats were purchased from National Rodent Laboratory Animal Resources (Shanghai, China). The animals were raised in a specific pathogen free barrier with free access to rodent sterile water and chow cubes. The barrier was a humidity and temperature-controlled environment with 12-hour light/dark cycles. All of the animal experiment protocols involved in this study were approved by the Ethics Committee on Animal Experimentation of East China Normal University (Shanghai, China).

Target-site selection

The sequence of *Ces2a* gene was obtained from NCBI (https://www.ncbi.nlm.nih.gov/pmc/). The gene ID (Ensembl) ENSRNOG00000011330 was submitted to the online website (https://benchling.com): CRISPR-CRISPR guides to import the sequence. The first exon sequence was selected for editing, and multiple 18 bp target sequence followed by a protospacer

Molecular Pharmacology Fast Forward. Published on September 9, 2021 as DOI: 10.1124/molpharm.121.000357
This article has not been copyedited and formatted. The final version may differ from this version.

adjacent motif (PAM) site (5'-NGG-3') in the 3' end was obtained. Two sequences, 5'-TCTCCTCCAGCATGTGCA-3' and 5'-TTGGCTAGACTTCCTGGT-3' located upstream of the gene, were selected as the editing target gene.

In vitro synthesis of sgRNA and Cas9 mRNA

Firstly, a 60 bp oligo fragment including the T7 promotor and *Ces2a* target sequence was synthesized. Based on this fragment, the sgRNA double-stranded template was constructed by overlapping PCR, and the products were then transcribed *in vitro* by the T7 transcription kit. Secondly, using the Cas9 plasmid as template, Cas9 mRNA was constructed according to the instructions of SP6 *in vitro* Transcription Kit. Both the sgRNA of *Ces2a* and Cas9 mRNA were extracted and purified by phenol-chloroform methods, and subsequently stored at -80℃ for further application.

Co-microinjection of sgRNA and Cas9 mRNA into zygote

Robust 8-week-old SD male rats were selected and caged with healthy 8-week-old SD female rats to collect fertilized eggs. The embryos were incubated in culture medium and 5% CO_2 for 2 h at 37℃. Then, the mixture of *Ces2a* sgRNA (25 ng/μL) and Cas9 mRNA (50 ng/μL) was co-microinjected into the cytoplasm of the embryos. The injected embryos were cultured in the incubator for 2 h, and the

Molecular Pharmacology Fast Forward. Published on September 9, 2021 as DOI: 10.1124/molpharm.121.000357
This article has not been copyedited and formatted. The final version may differ from this version.

surviving embryos with intact cytoplasmic membrane and normal perivitelline space were transplanted into the oviducts of the pseudo pregnant female rats.

Genotype identification

The genomic DNA was extracted from the toes of newborn rats, and then amplified by *Ces2a* primers (Table 1) with Easy-Taq DNA polymerase for identifying the genotypes of F0 chimeras with 1.5% agarose gel. PCR products with different bands were selected from wild-type (WT) rats for precise sequence and analyzed by DNAMAN (Lynnon Biosoft, San Ramon, CA, USA). The F0 offsprings carrying the expected mutations were caged with WT rats to obtain F1 generation. The genomic types of F1 rats were identified through direct sequencing of PCR products, and healthy adult F1 male and female rats with the same mutation were selected to mate to obtain F2 generation. The genomic types of F2 generation were identified by 1.5% agarose gel.

Off-target site validation

The information of *Ces2a* target-sites was submitted to the online website (https://benchling.com) to obtain potential off-target sites. Eight sites (Table 2) with relatively high off-targeting potential (score > 4.0) were selected for further analysis. Three homozygous KO rats and one WT rat were randomly selected for off-targeting

Molecular Pharmacology Fast Forward. Published on September 9, 2021 as DOI: 10.1124/molpharm.121.000357
This article has not been copyedited and formatted. The final version may differ from this version.

analysis sequencing. The primers are listed in Table 1. The sequencing results were analyzed in DNAMAN (Lynnon Biosof, San Ramon, CA, USA).

mRNA expression by PCR

Male *Ces2a* KO rats and WT rats (8 weeks old) were sacrificed by CO_2 asphyxiation. The liver and small intestine were collected and frozen at -80℃ for further experimentation. Each unit of liver or small intestine (0.1 g) was homogenized by Automatic Sample Rapid Grinding Instrument (JXFSTPRP-24, Shanghai, China). The total mRNA was extracted according to the instruction of the Trizol method and then reverse-transcribed into cDNA. The obtained cDNA was used for PCR by *Ces2a* primers (Table 1) with Taq enzyme system. And the agarose gel electrophoresis was performed to validate the PCR results.

Protein expression by LC-MS/MS

Each unit of liver (0.1 g) was added with 400 μL lysate, containing RIPA, protease inhibitor, phosphatase inhibitor and phenylmethanesulfonylfluoride and then samples were homogenized and pyrolyzed at 4℃ for 2 h to extract total protein. After enzymatic hydrolysis at 37℃ for 20 hours, samples were subsequently desalted and lyophilized, redissolved in 0.1% formic acid and stored at -20℃ for further use. Protein expression were detected by LC-MS/MS (Applied Protein Technology, shanghai, China). The mass-to-charge ratios of peptides and peptide fragments were

Molecular Pharmacology Fast Forward. Published on September 9, 2021 as DOI: 10.1124/molpharm.121.000357
This article has not been copyedited and formatted. The final version may differ from this version.

collected. Total 20 fragments were collected after each full scan Atlas (MS2 scan) for database search. The mass of carboxylic ester hydrolase sequence (containing *Ces2a, Ces2c, Ces2j*) was 1582.7416. The mobile phase consisted of H_2O (A) and acetonitrile (B), both containing 0.1% formic acid (*v/v*) and twenty fragments were collected after each full scan. Data were processed and analyzed by Proteome Discoverer 1.4 (Thermo Fisher Scientific, Waltham, MA, USA).

Detection of compensatory effects

Total RNA was extracted from liver and small intestine of WT and KO rats by Trizol method according to the guidelines. Then, the concentration was measured with nano-drop 2000 spectrophotometer (Thermo Fisher Scientific). The total RNA was quantitatively reverse-transcribed into cDNA by using the Takara RR036A kit. The main subtypes of carboxylesterase were detected by real-time quantitative PCR using Quant Studio 3 Real-Time PCR System (Thermo Fisher Scientific). The primer information is listed in Table 1. The β-actin was set as the internal reference.

Body weight

Male *Ces2a* $^{(-/-)}$ and WT rats were weighed once a week from the 3rd week to the 14th week. In addition, the liver weight at the age of 14 weeks was recorded.

Serum biochemical indexed detection

Molecular Pharmacology Fast Forward. Published on September 9, 2021 as DOI: 10.1124/molpharm.121.000357
This article has not been copyedited and formatted. The final version may differ from this version.

In order to detect whether there were some physiologic changes in *Ces2a* KO rats, male *Ces2a* $^{(-/-)}$ and WT rats (8 and 14 weeks old, respectively) fasted for 12h before serum collection and drank sterile water freely. Blood samples were collected from the tail vein, and the serum biochemical indexes were detected by Shanghai ADICON Clinical Laboratories (Shanghai, China). Liver function indicators include total protein (TP), albumin (ALB), globulin (GLB), albumin/globulin ratio (ALB/GLB), total bilirubin (TBL), direct bilirubin (DBL), indirect bilirubin (IBIL), aspartate aminotransferase (AST), alanine aminotransferase (ALT), aspartate aminotransferase/alanine aminotransferase (AST/ALT), alkaline phosphatase (ALP) and total bile acid (TBA). Blood lipid indexes include triglyceride (TG), total cholesterol (T-CH), high density lipoprotein cholesterol (HDL-C) and low density lipoprotein cholesterol (LDL-C).

Glucose and insulin tolerance test

Glucose (GLU), a commonly used indicator of physiological status, was also detected. In glucose tolerance test (GTT), male *Ces2a* $^{(-/-)}$ and WT rats (14 weeks old) fasted for 16 h with free access to sterile water. The glucose dissolved in sterilized saline was intraperitoneally injected into rats at a single dose of 2 g/kg. Blood samples were collected from tail vein both before injection and at 15, 30, 45, 60, 90, and 120 min after injection. The concentration of glucose was tested with blood glucose meter.

Molecular Pharmacology Fast Forward. Published on September 9, 2021 as DOI: 10.1124/molpharm.121.000357
This article has not been copyedited and formatted. The final version may differ from this version.

In the insulin tolerance test (ITT), male *Ces2a* $^{(-/-)}$ and WT rats (14 weeks old) fasted for 6 h and drank sterile water freely. Insulin dissolved in acidic saline and then diluted by sterilized saline was intraperitoneally injected into rats at a single dose of 1 IU/mL. Blood samples were collected from tail vein both before injection and at 15, 30, 45, 60, and 90 min after injection. Blood glucose concentration was measured by blood glucose meter.

Liver staining

Male *Ces2a* $^{(-/-)}$ and WT rats (8 and 14 weeks old) were sacrificed. Liver tissue was carefully separated, cut into small pieces (1 cm × 1 cm × 0.5 cm), fixed with 4% paraformaldehyde PBS buffer, embedded in paraffin for cutting into 3 μm sections, and stained with Haemotoxylin and Eosin (H&E), as well as Oil Red O according to the standard procedure.

Measurement of lipids in liver

Liver tissue (100 mg) from male *Ces2a* $^{(-/-)}$ rats at 14-week-old was homogenized with 300 μL methanol and then lipids was extracted with 600 μL chloroform at 4℃ for 12 h. The mixture was centrifuged under 12000 *g* for 20 min at 4 ℃. The supernatant was subsequently transferred into a new centrifuge tube and dried under the atmosphere of nitrogen. The precipitation was reconstituted with alcohol to extract lipids and followed by detection by ADICON Clinical Laboratories.

Molecular Pharmacology Fast Forward. Published on September 9, 2021 as DOI: 10.1124/molpharm.121.000357
This article has not been copyedited and formatted. The final version may differ from this version.

In vitro determination of Ces2a activity

The liver microsomes were prepared from 8-week-old male KO and WT rats, respectively. After comparing different protein concentrations and incubation time, we confirmed the optimal system. The incubation mixture included 0.5 mg/mL liver microsomes protein, as well as 20-1000 μM diltiazem. The mixture was incubated in a 0.1 M phosphate buffer system, and the final volume was 300 μL. After pre-incubating at 37℃ for 5 min, diltiazem was added to start the reaction. After incubation for 30 min, ice-cold acetonitrile (300 μL) containing 100 ng/mL verapamil (internal standard) was added to terminate the reaction. The mixture was centrifuged at 10,000 *g* at 4℃ for 15 min, and the supernatant was stored at -20℃ for subsequent experiments.

In vivo determination of Ces2a activity

The healthy 8-week-old male KO and WT rats were used in this study. The rats were given diltiazem at a single dose of 15 mg/kg (volume 5 mL/kg, dissolved in water) by gavage. Blood samples were collected from the tail vein at 0.08, 0.17, 0.5, 1, 2, 3, 4, 6, 8, 10, 12, and 24 h after administration. The blood samples were centrifuged at 10,000 *g* at 4℃ for 15 min, and the supernatant was stored at -20℃ for subsequent experiments.

Molecular Pharmacology Fast Forward. Published on September 9, 2021 as DOI: 10.1124/molpharm.121.000357
This article has not been copyedited and formatted. The final version may differ from this version.

Quantification of diltiazem and its metabolite by LC-MS/MS

The LC-MS/MS system consisted of an Agilent 1290 HPLC-6470 triple quadrupole mass spectrometer coupled with an Agilent Jet Stream ESI ion source (Agilent Technologies, Santa Clara, CA, USA). The chromatographic separation was performed on a Phenomenex Kinetex XB-C18 column (3 × 100 mm, 2.6 μm). The mobile phase consisted of H_2O (A) and acetonitrile (B), both containing 0.1% formic acid (*v/v*). Diltiazem metabolite and IS were eluted by HPLC gradient: 0 - 3 min, 20% - 70% B; 3 - 4 min, 70% B; 4 - 4.3 min, 70% - 20% B. The flow rate was 0.3 mL/min and the injection volume was 2 μL. Both diltiazem, deacetyldiltiazem and IS were monitored in positive ESI mode, with the ion transition of 415.1→165.1, 373.1→177.8 and 455.2→165.1, respectively.

Statistical data analysis

All data in this study were presented as mean ± standard deviation (mean ± SD). The data were analyzed by two-tailed t test. GraphPad Prism 8.0 (GraphPad Software Inc., San Diego, CA, USA) was used to plot mean plasma concentration-time curves. The pharmacokinetic parameters of diltiazem and its metabolite was calculated by WinNonlin 5.2.1 (Pharsight Corporation, Mountain View, CA, USA) based on the non-compartmental model. The significant difference was considered when $p < 0.05$, expressed as $*p < 0.05$, $**p < 0.01$, and $***p < 0.001$.

Molecular Pharmacology Fast Forward. Published on September 9, 2021 as DOI: 10.1124/molpharm.121.000357
This article has not been copyedited and formatted. The final version may differ from this version.

Results

Generation of Ces2a KO rats

After the co-injection of *Ces2a* sgRNA and Cas9 mRNA, a total of 27 neonatal rats were obtained. We randomly numbered these 27 rats of F0 generation from 1# to 27#. Then PCR and agarose gel electrophoresis were performed. As shown in Fig.1A, multiple mutant alleles were identified among these founders, numbered as 1#, 3#, 4#, 9#, 11#, 12#, 18#, 21#, 23#, 26#, 27#, indicating that a large fragment of the gene sequence had changed, which were then sequenced and analyzed. The peak patterns of 3#, 9#, 11#, 12#, 21#, 27# were in a state of disorder and cannot be analyzed. The remaining sequencing results are shown in Fig.1B. The rats with non-triple base number changes in the exon region were selected for subsequent experiments. Since there was 69bp deletion in 23# exon, F1 generation was obtained by crossing 1#, 4#, 18#, 26# with WT rats. The genomic DNA of F1 generation was sequenced and analyzed. Healthy male and female rats with the same mutation were selected for mating to obtain F2 generation. After analysis of PCR products of F2 rats with 1.5% agarose gel, individuals with a homozygous deletion were obtained (Supplementary information Fig. S1). In this study, KO rats after F2 generation were used for further study and all WT rats were littermate rats of the KO rats.

Off-target analysis

Molecular Pharmacology Fast Forward. Published on September 9, 2021 as DOI: 10.1124/molpharm.121.000357
This article has not been copyedited and formatted. The final version may differ from this version.

Since CRISPRP/Cas9 system allows 1-3 base pair mismatches in PAM-distal area, which may lead to off-target cleavage, the potential off-target sites were also detected. Three *Ces2a* KO rats were randomly selected to specifically amplify the potential off-target sites using 8 pairs of designed primers (Table 1) and then sent to sequencing analysis. The results showed that *Ces2a* gene-edited rats were off-target at OT-5 (Supplementary information Fig. S2). By searching the NCBI database, it was found that OT-5 did not belong to any gene. Therefore, there was no off-target in *Ces2a* KO rats.

Expression of Ces2a in WT and KO rats

The expression of *Ces2a* in the liver of WT and KO rats was detected at mRNA and protein levels, respectively. The results showed that the *Ces2a* mRNA was completely absent in the liver (Fig. 2A) and small intestine (Fig. 2B) of KO rats. At the same time, the results of protein showed that compared with WT rats, KO rats did not express carboxylic ester hydrolase, containing CES2A, CES2C and CES2J (Table 3). These results confirmed that the construction of *Ces2a* KO rat model was successful.

Compensatory expression of major carboxylesterases in WT and KO rats

In order to detect the compensatory expression of other major carboxylesterases after *Ces2a* gene knockout, we used real-time quantitative PCR to detect the mRNA

Molecular Pharmacology Fast Forward. Published on September 9, 2021 as DOI: 10.1124/molpharm.121.000357
This article has not been copyedited and formatted. The final version may differ from this version.

levels of major carboxylesterases in rats. The results showed that in the liver, compared with WT rats, the mean change in mRNA expression of *Ces1e*, *Ces1f* and *Ces1d* increased by about 98% (95% confidence interval [CI] 53%-143%, $p < 0.001$), 67% (95% CI 43%-93%, $p < 0.001$), and 66% (95% CI 19%-110%, $p < 0.05$), respectively, and the expression of *Ces2c* decreased by about 53% (95% CI 38%-69%, $p < 0.01$) in KO rats **(**Fig. 3A**)**. In the small intestine, the mRNA expression of *Ces1d* and *Ces2c* in KO rats also decreased by about 86% (95% CI 75%-97%, $p < 0.05$) and 52% (95% CI 35%-70%, $p < 0.01$), respectively **(**Fig. 3B**)**.

Physiological conditions detected in WT and KO rats

Compared with WT rats, the body weight of *Ces2a* KO rats was higher from the 6th week (Fig. 4A), the liver weight was higher too at the 14th week (Fig. 4B), and the organ coefficient (liver weight/body weight) was also increased (Fig. 4C). At the same time, the liver of 8-week-old and 14-week-old KO and WT rats were stained with H&E. There was no statistically significant difference at the 8th week, but obvious lipid vacuoles as well as eosinophils appeared in the liver of KO rats at the 14th week (Fig. 4D), the oil Red O staining also showed more reddish liver in KO rats at the 14th week (Fig. 4E), indicating that there was more fat accumulation in the liver of KO rats.

Glucose and insulin tolerance test

Molecular Pharmacology Fast Forward. Published on September 9, 2021 as DOI: 10.1124/molpharm.121.000357
This article has not been copyedited and formatted. The final version may differ from this version.

The areas under the curve (AUC) of GTT and ITT of 14-week-old KO rats were 34% (95% CI 18%-50%, $p < 0.01$) and 53% (95% CI 38%-67%, $p < 0.001$) higher than those of WT rats, respectively (Fig. 5). These results showed that glucose and insulin sensitivity of *Ces2a* KO rats were lower than those of 14-week-old WT rats, indicating that the deletion of *Ces2a* deteriorated the glucose tolerance and insulin resistance.

Clinical chemistry analysis of WT and KO rats

Due to the crucial role of *Ces2* in lipid metabolism, some important endogenous substances such as bile acids and lipids need to be detected. Moreover, if the *Ces2a* KO rats may be further used in the study of NAFLD, it is necessary to know whether the physiological indexes of *Ces2a* KO rats have changed and whether the growth and reproduction of KO rats are normal. WT and KO rats (8 and 14 weeks old) were randomly selected for serum tests of liver function. At the 8th week, serum biochemistry data showed that TBL, DBL, IBIL, AST/ALT, ALP, TBA, TG, T-CH, HDL-C and LDL-C levels of KO rats were all within 15% of the WT rats **(**Fig. 6A**)**. At the 14th week, however, the levels of TBL, DBL and IBIL in KO rats increased by 1.43-, 1.72- and 1.63-fold, respectively (Fig.6B). At the same time, the TBA increased significantly by 2.74-fold, and ALP increased by 1.25-fold. Moreover, the level of ALT in KO rats was higher than that of WT rats, and the level of AST/ALT was slightly lower than that of WT rats, indicating the occurrence of minor liver damage.

Molecular Pharmacology Fast Forward. Published on September 9, 2021 as DOI: 10.1124/molpharm.121.000357
This article has not been copyedited and formatted. The final version may differ from this version.

There was no statistically significant difference in TG level. However, T-CH, HDL-C and LDL-C all increased by nearly 1.50-fold, indicating the disorder of lipid metabolism, particularly cholesterol metabolism in KO rats (Fig. 6B). Except for the above indexes, liver protein synthesis levels of KO rats were all within 10% of WT (Data not shown). Lipids in liver of WT and KO rats at 14-week-old were also detected. TG and LDL-C in liver of KO rats were 1.49- and 1.89-fold higher than that in WT rats, respectively, with no statistically significant difference in T-CH and HDL-C level, indicating heavy hepatic fat accumulation (Fig. 6C).

Determination of Ces2a activity in WT and KO rats

It is reported that diltiazem is metabolized by CES2A to produce its deacetylated metabolites in rats (Kurokawa et al., 2015). Using diltiazem as the substrate, the activity of CES2A *in vitro* and *in vivo* was determined by LC-MS/MS. In rat liver microsomes (RLM) of both WT and KO rats, the capacity to metabolize diltiazem was detected (Fig. 7A). Compared with WT RLMs, V_{max} of diltiazem metabolism in KO RLMs (1.03 ± 0.47 nmoL/min/mg protein) was decreased by 87% compared with WT rats (7.78 ± 0.35 nmoL/min/mg protein) (Fig. 7B), and the intrinsic clearance (C_{Lint}) of KO rats (0.54 ± 0.01 mL/min/kg) was also significantly reduced by 98% compared with WT rats (30.88 ± 0.51 mL/min/kg) (Fig. 7C). The results showed that compared with WT rats, the metabolic capacity of diltiazem *in vitro* in KO rats was significantly decreased.

Molecular Pharmacology Fast Forward. Published on September 9, 2021 as DOI: 10.1124/molpharm.121.000357
This article has not been copyedited and formatted. The final version may differ from this version.

To further assess the damaged function of CES2A *in vivo* in KO rats, pharmacokinetic experiments of diltiazem were carried out in WT and KO rats. After oral administration of diltiazem, there was no statistically significant difference between WT and KO rats (Fig. 7D). However, the PK parameters of deacetyldiltiazem showed crucial variation. Compared with WT rats, the maximum concentration (C_{max}) and $AUC_{0\text{-}24h}$ of KO rats were reduced by 98.7% and 97.3%, respectively (Table 4) (Fig. 7E). In addition, the mean residence time (MRT) of KO rats increased by 78.0% compared with those in WT rats. The pharmacokinetic results of diltiazem *in vivo* were consistent with the data *in vitro*, which further confirmed the loss of function of CES2A in KO rats.

Discussion

In recent years, more and more attention has been paid to CES2, as it plays an important role in endogenous and exogenous metabolism (Di, 2019; Frank et al., 1986; Song et al., 2019; Yi et al., 2019). Due to the defects of *in vitro* and *in vivo* models, the study of CES2 is greatly limited. Cell models *in vitro* include primary cell and Caco-2 cell models (Di, 2019). The primary stem cell model has a complete metabolic enzyme system, which can simulate the physiological environment of the body to a certain extent, but the cell culture conditions are strict and lack of regulatory pathways (LeCluyse, 2001; Zhang et al., 2019). Additionally, the expression of CES2 in Caco-2 cell line is very different from that in humans, which cannot reflect the real situation

Molecular Pharmacology Fast Forward. Published on September 9, 2021 as DOI: 10.1124/molpharm.121.000357
This article has not been copyedited and formatted. The final version may differ from this version.

of humans (Imai and Ohura, 2010; Ishizaki et al., 2018). *In vivo* models include inhibitor inhibiting transporter activity and gene editing model. However, the low specificity, high cost and potential cytotoxicity of inhibitors make the results unreliable (Takahashi et al., 2009).

Gene editing model has attracted much attention because of its clearer genetic background and better reflecting the function of CES2. In 2019, intestine-specific *Ces2c* overexpression mice were generated for studying the function of intestinal *Ces2c* (Maresch et al., 2019). However, there is still no rat model of *Ces2* gene deletion. Compared with mice, rats have larger body size, stronger tolerance, as well as sufficient blood volume, and they are suitable for studying physiological characteristics. In brief, the rat is a distinguished animal model for pharmacokinetic and toxicological studies (Ma et al., 2020; Wang et al., 2016). Compared with the early gene knockout technology based on homologous recombination, CRISPR/Cas9 system has the advantages of high efficiency, simple operation, short circle, low cost and high success rate, greatly accelerating the development of gene editing (Cong et al., 2013; Lu et al., 2021; Wang et al., 2017). Therefore, CRISPR/Cas9 technology was the first choice for the construction of *Ces2a* KO rat model in this study.

Compared with WT rats, there was no expression of *Ces2a* mRNA in the liver of KO rats. Meanwhile, the expression of protein group (containing CES2A, CES2C and CES2J) was also absent in the liver. In fact, at the mRNA expression level, *Ces2a*, *Ces2c* and *Ces2e* are expressed in rat liver, while *Ces2j* is undetectable (Ohura et al.,

Molecular Pharmacology Fast Forward. Published on September 9, 2021 as DOI: 10.1124/molpharm.121.000357
This article has not been copyedited and formatted. The final version may differ from this version.

2014; Sanghani et al., 2002). Moreover, the deletion of *Ces2a* caused the decreased mRNA expression of *Ces2c*, which may cause the reduced protein expression of CES2C in the KO rat. As a result, the deletion of *Ces2a*, no measurable level of *Ces2j*, as well as decreased protein expression of CES2C led to the absence of protein group (containing CES2A, CES2C and CES2J) in liver of KO rats. Combined with the absence of *Ces2a* in the liver and small intestine of KO rats in mRNA level, *Ces2a* KO rats were successfully generated. Our original goal was to knock out *Ces2a*, but unexpectedly decreased the expression of *Ces2c* and *Ces2j*. Such a model may be more conducive to the study the function of CES2. In addition, human blood lacks CES activity, while plasma derived from rodent is very proficient at CES substrate activation. Hence, animal models designed to predict tumor responses in humans may overestimate the efficacy of the drug due to the increased CES activity (Morton et al., 2005). Compared with conditional knockout rat model, our *Ces2a* KO rats may represent a more accurate model for drug metabolism.

Since CES2 was age-dependent (Hines et al., 2016), liver H&E staining and serum physiological indexes of liver function were detected in 8- and 14-week-old rats. There was no significant difference of the baseline body weights between WT and KO rats, however, during the course of this study, KO rats showed continuous weight gain and were finally significantly heavier than WT rats, showing the characteristic of obesity. Meanwhile, the H&E and Oil Red O staining of rats at 14-week-old showed heavy fat accumulation, minor eosinophils as well as

Molecular Pharmacology Fast Forward. Published on September 9, 2021 as DOI: 10.1124/molpharm.121.000357
This article has not been copyedited and formatted. The final version may differ from this version.

enlargement of hepatic sinusoids in KO rats, which confirmed the hepatic fat accumulation. To further explored the influence of *Ces2a* on liver, subsequent tests were conducted on 14-week-old rats and the results showed that glucose and insulin sensitivity of *Ces2a* KO rats were significantly lower than those of 14-week-old WT rats, indicating the loss of *Ces2a* deteriorated the glucose tolerance and insulin resistance. At the same time, the results of physiological indexes showed that AST/ALT decreased in KO rats, suggesting the liver damage occurred in KO rats at 14-week-old. In addition, T-CH, LDL-C, TBA and ALP in 14-week-old KO rats were significantly higher than those in WT rats, indicating that the loss of *Ces2a* led to the disorder of cholesterol metabolism, which may also be the cause of hepatic fat accumulation and liver injury. Surprisingly, the level of HDL-C was also significantly up-regulated. In order to maintain the balance of cholesterol, the body needs to produce more HDL-C and bring the excess cholesterol deposited in the peripheral tissue back to the liver to regulate redistribution of cholesterol. Hepatic lipids detection showed that significantly increased TG and LDL-C level in KO rats at 14-week-old, which was consistent with the serum detection. These results suggested that KO rats showed the features of obesity, hyperglycemia/insulin resistance and hepatic fat accumulation, which were also characteristics of an ideal NAFLD model (Jahn et al., 2019). The close relationship between *Ces2a* and lipid metabolism may lead to the occurrence of NAFLD. Moreover, with the increase of age, *Ces2a* is more

Molecular Pharmacology Fast Forward. Published on September 9, 2021 as DOI: 10.1124/molpharm.121.000357
This article has not been copyedited and formatted. The final version may differ from this version.

involved in the metabolism of endogenous substances. However, the regulatory effect of *Ces2a* on lipid metabolism remains to be further studied.

We further used diltiazem, a selective substrate of CES2A, to verify the change of its function in KO rats. In humans, diltiazem is primarily metabolized to *N*-demethyldiltiaze, *O*-demethylditiazem and deacetyldiltiazem through CYP3A4, CYP2D6, and esterase. The AUC ration of the metabolites is 1:3.4:28, respectively (Molden et al., 2002). Although esterase plays an important role in the deacetylation of diltiazem, it has not been identified so far. Previous studies have reported that four carboxylesterase enzymes (CES1D, CES1E, CES1F and CES2A) in rats are identified as potential candidate deacetylases of diltiazem, but the CES2A enzyme is considered to be the main enzyme responsible for diltiazem deacetylation (Kurokawa et al., 2015). Therefore, although the compensatory effects were observed in KO rats, the deacetylase of diltiazem by CES2A in RLM was not affected. Both *in vitro* and *in vivo* experiments demonstrated the loss of function of CES2A in KO rats.

At present, different animal models have been constructed to simulate NAFLD, such as genetic model, nutrient-deficient model and models based on obesogenic high-fat diets. However, these models are limited by the disadvantages of overly artificial diets, vague genetic background or unclear epidemiology (Jahn et al., 2019). Since there is no approved drug for NAFLD, there is an urgent need to identify promising pharmacological targets and develop future therapies. Our *Ces2a* KO rats have the characteristics of obesity, hyperglycemia, insulin resistance and hepatic fat

Molecular Pharmacology Fast Forward. Published on September 9, 2021 as DOI: 10.1124/molpharm.121.000357
This article has not been copyedited and formatted. The final version may differ from this version.

accumulation, which may be an ideal NAFLD model. It has the advantages of clear genetic background, clear epidemiology, short feeding period and no additional artificial diets.

In conclusion, the *Ces2a* KO rat model was successfully established by CRISPR/Cas9 technology for the first time. This model can be used in the study of drug metabolism and pharmacokinetics. At the same time, it has the characteristics related to NAFLD, and is a good disease model for the study of NAFLD. Using this animal model, we can better understand the role of CES2 in drug metabolism and lipid metabolism.

Author contributions

Participated in research design: Wang.

Conducted experiments: J Liu, Shang, Huang and Xu.

Performed data analysis: J Liu, Shang, Z Liu and Wang.

Wrote or contributed to the drafting of the manuscript: J Liu, Lu, Zhang and Wang.

References

Abdelwahab NS, Elshemy HAH and Farid NF (2018) Determination of flutamide and two major metabolites using HPLC-DAD and HPTLC methods. *Chem Cent J* **12**(1): 4.

Boberg M, Vrana M, Mehrotra A, Pearce RE, Gaedigk A, Bhatt DK, Leeder JS and Prasad B (2017) Age-Dependent Absolute Abundance of Hepatic Carboxylesterases (CES1 and CES2) by LC-MS/MS Proteomics: Application to PBPK Modeling of Oseltamivir In Vivo Pharmacokinetics in Infants. *Drug Metab Dispos* **45**(2): 216-223.

Cong L, Ran FA, Cox D, Lin S, Barretto R, Habib N, Hsu PD, Wu X, Jiang W, Marraffini LA and Zhang F (2013) Multiplex genome engineering using CRISPR/Cas systems. *Science* **339**(6121): 819-823.

Di L (2019) The Impact of Carboxylesterases in Drug Metabolism and Pharmacokinetics. *Curr Drug Metab* **20**(2): 91-102.

Fleming CD, Edwards CC, Kirby SD, Maxwell DM, Potter PM, Cerasoli DM and Redinbo MR (2007) Crystal structures of human carboxylesterase 1 in covalent complexes with the chemical warfare agents soman and tabun. *Biochemistry* **46**(17): 5063-5071.

Frank N, Caesar R, Scherf HR and Wiessler M (1986) Influence of the carboxylesterase inhibitor bis-p-nitrophenylphosphate on the rates of hydrolysis of various alpha-esters of 1-(N-methyl-N-nitrosamino)-methanol in vitro and in vivo and on the acute toxicity and carcinogenicity of 1-(N-methyl-N-nitrosamino)-methylacetate. *J Cancer Res Clin Oncol* **111**(2): 98-102.

Furihata T, Hosokawa M, Masuda M, Satoh T and Chiba K (2006) Hepatocyte

nuclear factor-4alpha plays pivotal roles in the regulation of mouse carboxylesterase 2 gene transcription in mouse liver. *Arch Biochem Biophys* **447**(2): 107-117.

Hines RN, Simpson PM and McCarver DG (2016) Age-Dependent Human Hepatic Carboxylesterase 1 (CES1) and Carboxylesterase 2 (CES2) Postnatal Ontogeny. *Drug Metab Dispos* **44**(7): 959-966.

Holmes RS, Wright MW, Laulederkind SJ, Cox LA, Hosokawa M, Imai T, Ishibashi S, Lehner R, Miyazaki M, Perkins EJ, Potter PM, Redinbo MR, Robert J, Satoh T, Yamashita T, Yan B, Yokoi T, Zechner R and Maltais LJ (2010) Recommended nomenclature for five mammalian carboxylesterase gene families: human, mouse, and rat genes and proteins. *Mamm Genome* **21**(9-10): 427-441.

Hryhorowicz M, Lipinski D, Zeyland J and Slomski R (2017) CRISPR/Cas9 Immune System as a Tool for Genome Engineering. *Arch Immunol Ther Exp (Warsz)* **65**(3): 233-240.

IMAI T (2006) Human Carboxylesterase Isozymes Catalytic Properties and Rational Drug Design. *Drug Metabolism and pharmacokinetics* **21**: 173-185.

Imai T and Ohura K (2010) The role of intestinal carboxylesterase in the oral absorption of prodrugs. *Curr Drug Metab* **11**(9): 793-805.

Ishizaki Y, Furihata T, Oyama Y, Ohura K, Imai T, Hosokawa M, Akita H and Chiba K (2018) Development of a Caco-2 Cell Line Carrying the Human

Intestine-Type CES Expression Profile as a Promising Tool for Ester-Containing Drug Permeability Studies. *Biol Pharm Bull* **41**(5): 697-706.

Jahn D, Kircher S, Hermanns HM and Geier A (2019) Animal models of NAFLD from a hepatologist's point of view. *Biochim Biophys Acta Mol Basis Dis* **1865**(5): 943-953.

Kamendulis LM, Brzezinski MR, Pindel EV, Bosron WF and Dean RA (1996) Metabolism of cocaine and heroin is catalyzed by the same human liver carboxylesterases. *J Pharmacol Exp Ther* **279**(2): 713-717.

Kim KK, Song HK, Shin DH, Hwang KY, Choe S, Yoo OJ and Suh SW (1997) Crystal structure of carboxylesterase from Pseudomonas fluorescens, an alpha/beta hydrolase with broad substrate specificity. *Structure* **5**(12): 1571-1584.

Kurokawa T, Fukami T and Nakajima M (2015) Characterization of Species Differences in Tissue Diltiazem Deacetylation Identifies Ces2a as a Rat-Specific Diltiazem Deacetylase. *Drug Metab Dispos* **43**(8): 1218-1225.

Laizure SC, Herring V, Hu Z, Witbrodt K and Parker RB (2013) The role of human carboxylesterases in drug metabolism: have we overlooked their importance? *Pharmacotherapy* **33**(2): 210-222.

LeCluyse EL (2001) Human hepatocyte culture systems for the in vitro evaluation of cytochrome P450 expression and regulation. *Eur J Pharm Sci* **13**(4): 343-368.

Li Y, Zalzala M, Jadhav K, Xu Y, Kasumov T, Yin L and Zhang Y (2016)

Carboxylesterase 2 prevents liver steatosis by modulating lipolysis, endoplasmic reticulum stress, and lipogenesis and is regulated by hepatocyte nuclear factor 4 alpha in mice. *Hepatology* **63**(6): 1860-1874.

Lian J, Nelson R and Lehner R (2018) Carboxylesterases in lipid metabolism: from mouse to human. *Protein Cell* **9**(2): 178-195.

Lu J, Liu J, Guo Y, Zhang Y, Xu Y and Wang X (2021) CRISPR-Cas9: A method for establishing rat models of drug metabolism and pharmacokinetics. *Acta Pharmaceutica Sinica B.*

Ma SF, Anraku M, Iwao Y, Yamasaki K, Kragh-Hansen U, Yamaotsu N, Hirono S, Ikeda T and Otagiri M (2005) Hydrolysis of angiotensin II receptor blocker prodrug olmesartan medoxomil by human serum albumin and identification of its catalytic active sites. *Drug Metab Dispos* **33**(12): 1911-1919.

Ma X, Shang X, Qin X, Lu J, Liu M and Wang X (2020) Characterization of organic anion transporting polypeptide 1b2 knockout rats generated by CRISPR/Cas9: a novel model for drug transport and hyperbilirubinemia disease. *Acta Pharm Sin B* **10**(5): 850-860.

Maresch LK, Benedikt P, Feiler U, Eder S, Zierler KA, Taschler U, Kolleritsch S, Eichmann TO, Schoiswohl G, Leopold C, Wieser BI, Lackner C, Rulicke T, van Klinken J, Kratky D, Moustafa T, Hoefler G and Haemmerle G (2019) Intestine-Specific Overexpression of Carboxylesterase 2c Protects Mice From Diet-Induced Liver Steatosis and Obesity. *Hepatol Commun* **3**(2): 227-245.

Molden E, Johansen PW, Boe GH, Bergan S, Christensen H, Rugstad HE, Rootwelt H, Reubsaet L and Lehne G (2002) Pharmacokinetics of diltiazem and its metabolites in relation to CYP2D6 genotype. *Clin Pharmacol Ther* **72**(3): 333-342.

Morton CL, Iacono L, Hyatt JL, Taylor KR, Cheshire PJ, Houghton PJ, Danks MK, Stewart CF and Potter PM (2005) Activation and antitumor activity of CPT-11 in plasma esterase-deficient mice. *Cancer Chemoth Pharm* **56**(6): 629-636.

Nishikawa K, Naka T, Chatani F and Yoshimura Y (1997) Candesartan cilexetil: a review of its preclinical pharmacology. *J Hum Hypertens* **11 Suppl 2**: S9-17.

Oda S, Fukami T, Yokoi T and Nakajima M (2015) A comprehensive review of UDP-glucuronosyltransferase and esterases for drug development. *Drug Metab Pharmacokinet* **30**(1): 30-51.

Ohura K, Tasaka K, Hashimoto M and Imai T (2014) Distinct patterns of aging effects on the expression and activity of carboxylesterases in rat liver and intestine. *Drug Metab Dispos* **42**(2): 264-273.

Ruby MA, Massart J, Hunerdosse DM, Schonke M, Correia JC, Louie SM, Ruas JL, Naslund E, Nomura DK and Zierath JR (2017) Human Carboxylesterase 2 Reverses Obesity-Induced Diacylglycerol Accumulation and Glucose Intolerance. *Cell Rep* **18**(3): 636-646.

Sanghani SP, Davis WI, Dumaual NG, Mahrenholz A and Bosron WF (2002) Identification of microsomal rat liver carboxylesterases and their activity with

retinyl palmitate. *Eur J Biochem* **269**(18): 4387-4398.

Sato Y, Miyashita A, Iwatsubo T and Usui T (2012) Simultaneous absolute protein quantification of carboxylesterases 1 and 2 in human liver tissue fractions using liquid chromatography-tandem mass spectrometry. *Drug Metab Dispos* **40**(7): 1389-1396.

Satoh T and Hosokawa M (2006) Structure, function and regulation of carboxylesterases. *Chem Biol Interact* **162**(3): 195-211.

Song YQ, Guan XQ, Weng ZM, Wang YQ, Chen J, Jin Q, Fang SQ, Fan B, Cao YF, Hou J and Ge GB (2019) Discovery of a highly specific and efficacious inhibitor of human carboxylesterase 2 by large-scale screening. *Int J Biol Macromol* **137**: 261-269.

Staudinger JL, Xu C, Cui YJ and Klaassen CD (2010) Nuclear receptor-mediated regulation of carboxylesterase expression and activity. *Expert Opin Drug Metab Toxicol* **6**(3): 261-271.

Takahashi S, Katoh M, Saitoh T, Nakajima M and Yokoi T (2009) Different inhibitory effects in rat and human carboxylesterases. *Drug Metab Dispos* **37**(5): 956-961.

Torres-Ruiz R and Rodriguez-Perales S (2017) CRISPR-Cas9 technology: applications and human disease modelling. *Brief Funct Genomics* **16**(1): 4-12.

Wang HX, Li M, Lee CM, Chakraborty S, Kim HW, Bao G and Leong KW (2017) CRISPR/Cas9-Based Genome Editing for Disease Modeling and Therapy:

Challenges and Opportunities for Nonviral Delivery. *Chem Rev* **117**(15): 9874-9906.

Wang X, Tang Y, Lu J, Shao Y, Qin X, Li Y, Wang L, Li D and Liu M (2016) Characterization of novel cytochrome P450 2E1 knockout rat model generated by CRISPR/Cas9. *Biochem Pharmacol* **105**: 80-90.

Xu G, Zhang W, Ma MK and McLeod HL (2002) Human carboxylesterase 2 is commonly expressed in tumor tissue and is correlated with activation of irinotecan. *Clin Cancer Res* **8**(8): 2605-2611.

Yi J, Bai R, An Y, Liu TT, Liang JH, Tian XG, Huo XK, Feng L, Ning J, Sun CP, Ma XC and Zhang HL (2019) A natural inhibitor from Alisma orientale against human carboxylesterase 2: Kinetics, circular dichroism spectroscopic analysis, and docking simulation. *Int J Biol Macromol* **133**: 184-189.

Zhang L, Liang C, Xu P, Liu M, Xu F and Wang X (2019) Characterization of in vitro Mrp2 transporter model based on intestinal organoids. *Regul Toxicol Pharmacol* **108**: 104449.

Footnotes

This work was supported in whole or part by grants from the National Natural Science Foundation of China (No. 81773808), the Science and Technology Commission of Shanghai Municipality (No. 18430760400), the China Postdoctoral Science Foundation (No. 2020M671051), the Fundamental Research Funds for the Central Universities and the Clinical Advantage Discipline of Health System of Putuo

Molecular Pharmacology Fast Forward. Published on September 9, 2021 as DOI: 10.1124/molpharm.121.000357
This article has not been copyedited and formatted. The final version may differ from this version.

District in Shanghai. This work was also supported from ECNU Multifunctional Platform for Innovation (011) and the Instruments Sharing Platform of School of Life Sciences, East China Normal University.

Molecular Pharmacology Fast Forward. Published on September 9, 2021 as DOI: 10.1124/molpharm.121.000357
This article has not been copyedited and formatted. The final version may differ from this version.

Table 1. Primer pairs used in this research

No.	Primer Name	Primer Sequence (5'-3')
1	*Ces2a*-F	CTGCTGGCTATTGGCTTCC
	Ces2a-R	CCTGCTGCTTTCCATCCC
2	*Ces2a*-OT-1-F	TCTCGATTACTTTTATAGACAC
	Ces2a-OT-1-R	CAGGGAAGGATACACCAT
3	*Ces2a*-OT-2-F	CTTTGAGATTATAGTGGGTT
	Ces2a-OT-2-R	AGATGGCCTACATCCTTA
4	*Ces2a*-OT-3-F	TTCCATCCCATAGGTTCA
	Ces2a-OT-3-R	GTGCCTTTGCTCTGACTG
5	*Ces2a*-OT-4-F	TTCAATAAGAACTTTGTCCCTC
	Ces2a-OT-4-R	CCCGGTTAATTTAAGCAGTA
6	*Ces2a*-OT-5-F	CTCAGAAGGACCAAGAAA
	Ces2a-OT-5-R	ATAGCCTAAGCTAAGGGA
7	*Ces2a*-OT-6-F	CTTGGTAGCTGGTGAGTC
	Ces2a-OT-6-R	TCCTATGGCTTCTGTCTT
8	*Ces2a*-OT-7-F	TTCCTCCTTCAGTTCCAC
	Ces2a-OT-7-R	GAGTTCCCACCTTCAAAA
9	*Ces2a*-OT-8-F	TTGGCAGAGCAGCATCAT
	Ces2a-OT-8-R	TGGCAGGAACCTCACAGA
10	*Ces1c*-F	ACTACAAACCTGGACAAGAAG
	Ces1c-R	GCAGTACCACTCCATCAATC
11	*Ces1d*-Q-F	CACTTCTGCTCTGATTACAAC
	Ces1d-Q-R	GGTTTCCAAGTAAATCCAG
12	*Ces1e*-Q-F	TCAATGACCTTCTAACTAACCG
	Ces1e-Q-R	TGGATGCCCCACCTAACACTAG
13	*Ces1f*-Q-F	CCTTCCTGGATTGTTAACC
	Ces1f-Q-R	TTATCCCTTTGTGAACTGAG
14	*Ces2a*-Q-F	CCTGCTTATTCTTATCCATGTG
	Ces2a-Q-R	GCCTACTTCATCCAGCATAT
15	*Ces2c*-Q-F	TAGCCCGACGAACTGAGA
	Ces2c-Q-R	GTCCTGACCCCACACATGG
16	*Ces2e*-Q-F	CTTTGCCAAGCCTCCTATAG
	Ces2e-Q-R	GTGGGCTGGTGTGTAGATGC
17	*Ces2h*-Q-F	GGATGTGAGCAGGTGGACTC
	Ces2h-Q-R	CTTCTTGGAGTCAGTGGTGG
18	*Ces2i*-Q-F	CTACAGACTGATATAATGAAGG
	Ces2i-Q-R	GTCCAGGTATCCCCAGTTGC
19	*Ces2j*-Q-F	GAATTGACCAAGCTTCCTATG
	Ces2j-Q-R	GTCCAGGTATCCCCAGTTGC
20	*Ces3a*-Q-F	CCTTATGGAAGTGCCCCCTG

Molecular Pharmacology Fast Forward. Published on September 9, 2021 as DOI: 10.1124/molpharm.121.000357
This article has not been copyedited and formatted. The final version may differ from this version.

	Ces3a-Q-R	AGGCTGACTTGAACTTCGCA
21	*β-actin*-Q-F	AGATCAAGATCATTGCTCCTCCT
	β-actin-Q-R	ACGCAGCTCAGTAACAGTCC

Molecular Pharmacology Fast Forward. Published on September 9, 2021 as DOI: 10.1124/molpharm.121.000357
This article has not been copyedited and formatted. The final version may differ from this version.

Table 2. Details for all potential off-target sites

Name	Chromosome	Spacer	PAM	Off-target
Ces2a sgRNA1	chr19	TTGGCTAGACTTCCTGGT	TGG	
Ces2a-OT-1	chr6	TGGACTAGACTTCCTGGT	GGG	5.5
Ces2a-OT-2	chr3	TTGTCTAGACTTCCTGCT	AAG	4.3
Ces2a sgRNA2	chr19	TCTCCTCCAGCATGTGCA	CGG	
Ces2a-OT-3	chr1	TCTGCTCCAGCATGTGCA	TGG	100
Ces2a-OT-4	chr19	TCTGCTCCAGCATGTGCA	TAG	100
Ces2a-OT-5	chr19	TCTCCTCCAGCATGTGCA	CGG	100
Ces2a-OT-6	chr19	TCTGCTCCAGCATGTGCA	TAG	100
Ces2a-OT-7	chr6	CCTCCTCAAGCATGTGCA	TAG	7.1
Ces2a-OT-8	chr1	CCTCCTGCAGCATGTGCA	TGG	4.6

Molecular Pharmacology Fast Forward. Published on September 9, 2021 as DOI: 10.1124/molpharm.121.000357
This article has not been copyedited and formatted. The final version may differ from this version.

Table 3. Information on CES2A protein expression by LC-MS/MS

Name	**Data**
Mass	1582.7416
Gene names	*Ces2a; Ces2c; Ces2j*
Protein names	Carboxylic ester hydrolase
Intensity KO	0
Intensity WT	106550000
iBAQ KO	0
iBAQ WT	5607700
LFQ intensity KO	0
LFQ intensity WT	84023000

Molecular Pharmacology Fast Forward. Published on September 9, 2021 as DOI: 10.1124/molpharm.121.000357
This article has not been copyedited and formatted. The final version may differ from this version.

Table 4 Pharmacokinetic parameters of deacetyldiltiazem after oral administration of diltiazem

Parameters	**Unit**	**WT rats**	**KO rats**
$T_{1/2}$	h	2.94 ± 0.72	2.45 ± 0.27
T_{max}	h	0.25	0.50
C_{max}	ng/mL	438.75 ± 138.04	5.69 ± 3.27***
$AUC_{0\text{-}24h}$	h*ng/mL	597.89 ± 91.89	15.66 ± 4.52***
$AUC_{0\text{-}inf}$	h*ng/mL	598.09 ± 92.01	15.74 ± 4.52***
$MRT_{0\text{-}24h}$	h	1.59 ± 0.12	2.83 ± 0.44**

The dose of diltiazem was 15 mg/kg (p.o.). Results were mean ± SD of six rats. $^{**}p < 0.01$ and $^{***}p < 0.001$ compared to WT rats.

Molecular Pharmacology Fast Forward. Published on September 9, 2021 as DOI: 10.1124/molpharm.121.000357
This article has not been copyedited and formatted. The final version may differ from this version.

Figure legends:

Fig. 1 Genotyping of the F0 generation of *Ces2a* KO rats generated by CRISPR/Cas9 system. (A) The mutations in F0 generation for *Ces2a* was detected by 1.5% agarose gel using PCR products amplified from F0 rat toes genomic DNA by Primer. "↓", mutation band. WT, wild type as negative control. (B) Analysis of *Ces2a* gene sequence of part of F0 generation rats. Four TA clones of the PCR products amplified from each F0 rat were sequenced. ".", nucleotide deletion. Green words, nucleotide insertion. "△", the number of changed nucleotide.

Fig. 2 Analysis of *Ces2a* expression in WT and KO rats (n = 3). (A) PCR analysis of *Ces2a* mRNA expression in liver of WT and KO rats. (B) PCR analysis of *Ces2a* mRNA expression in small intestine of WT and KO rats.

Fig. 3 Compensatory expression of other main *Ces* isoforms in *Ces2a* KO rats. (A) Compensatory expression in the liver. (B) Compensatory expression in the small intestine. All data were expressed as mean ± SD (n = 6). *$p < 0.05$, **$p < 0.01$, and ***$p < 0.001$ compared to WT group.

Fig. 4 (A) Body weight of WT and *Ces2a* KO rats from the 3rd week to the 14th week. Body weight was recorded once a week (n = 8). (B) Liver weight at the 14th week. Liver weight was determined and compared between WT and KO rats (n = 8) at 14 weeks of age. (C) Organ coefficient of liver. The liver organ coefficients of WT and KO rats were measured and compared. The ratio of Liver weight/Body weight was determined as the organ coefficient of liver. The results were shown as mean ± SD (n

= 8). (D) Haematoxylin & Eosin staining on liver sections from WT and KO rats at 14 weeks (n = 6). (E) Oil Red O staining on liver sections from WT and KO rats at 14 weeks (n = 6). "↓", lipid vacuoles, "▼" , eosinophils. *p < 0.05, **p < 0.01, and ***p < 0.001.

Fig. 5 Glucose and insulin tolerance of WT and *Ces2a* KO rats. (A, B) Glucose tolerance and area under the curve (AUC) of GTT in WT and KO rats at 14 weeks of age. Serum samples were collected at 15, 30, 45, 60, 90, and 120 min after intraperitoneal injection of a dose of 2 g/kg glucose. (C, D) Insulin sensitivity and area under the curve (AUC) of ITT in WT and KO rats at 14 weeks of age. Serum samples were collected at 15, 30, 45, 60, and 90 min after intraperitoneal injection of a single dose of 1 IU/mL insulin. The results were shown as mean ± SD of six rats. **p < 0.01, and ***p < 0.001.

Fig. 6 Physiological phenotype of *Ces2a* KO rats. (A) Clinical chemistry and physiological analysis of serum from male WT and KO rats at 8 weeks old. (B) Clinical chemistry and physiological analysis of serum from male WT and KO rats at 14 weeks old. (C) Hepatic lipids of WT and KO rats at 14 weeks old. High-density lipoproteins-cholesterol (HDL-C), low-density lipoproteins-cholesterol (LDL-C), triglycerides (TG), total cholesterol (TCH), total bile acid (TBA), aspartate amino transferase (AST), alanine amino transferase (ALT), alkaline phosphatase (ALP), total bilirubin (TBL), direct bilirubin (DBL), and direct bilirubin (DBIL) were compared

Molecular Pharmacology Fast Forward. Published on September 9, 2021 as DOI: 10.1124/molpharm.121.000357
This article has not been copyedited and formatted. The final version may differ from this version.

between WT and KO rats. The results were shown as mean ± SD of six rats. *$p < 0.05$, **$p < 0.01$, and ***$p < 0.001$.

Fig. 7 CES2A-mediated catalytic activity of WT and KO rats *in vitro* and *in vivo*. (A) *In vitro* metabolism of diltiazem, a substrate of CES2A, by WT and KO rat liver microsomes (RLM). The x-axis represents the concentration of diltiazem. The y-axis represents the metabolic velocity of CES2A. (B) The V_{max} comparison of diltiazem metabolism in WT and KO RLM. (C) The intrinsic clearance comparison of diltiazem metabolite in WT and KO RLM. (D) The concentration versus time profiles on pharmacokinetics of diltiazem in WT and KO rats. (E) The concentration versus time profiles on pharmacokinetics of deacetyldiltiazem in WT and KO rats. All data were expressed as mean ± SD of six rats in each group. $^{***}p < 0.001$ compared to WT rats.

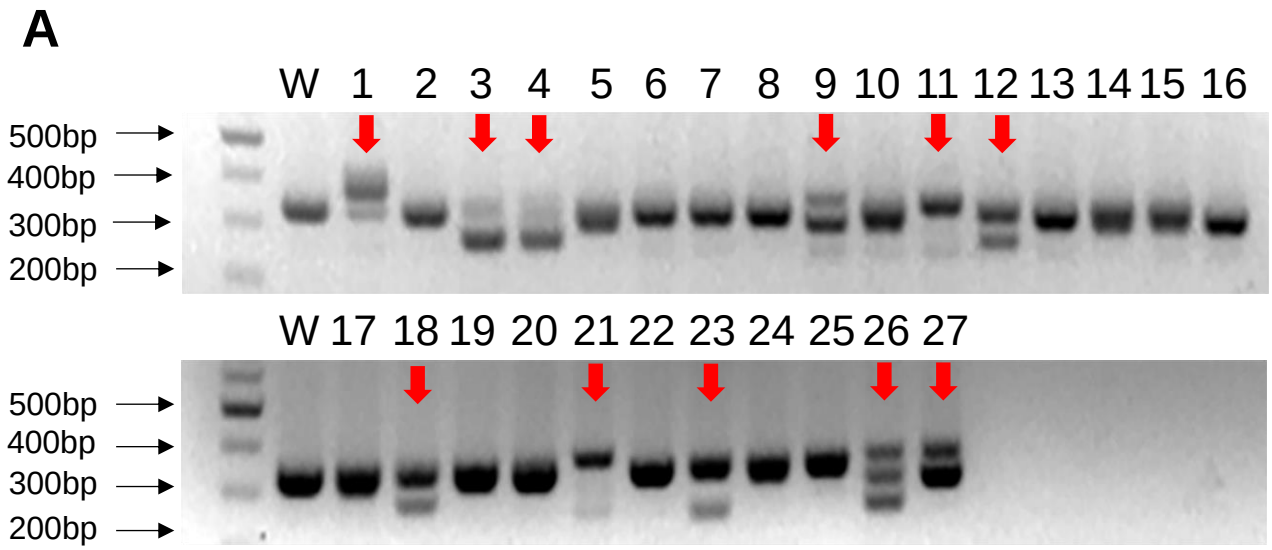

B

Ces2a	*Protospacer* PAM *Protospacer* PAM	
No.	ATGCCT*TTGGCTAGACTTCCTGGT*TGGCTGTATGTTGTAGCCTGTGGGCTCCTGCT*TCTCCTCCAGCATGTGCA*CGGTGAGACTGT	**WT**
1#	ATGCCT*TTGGCTAGACTTCCTGGT*TGGCTGTATGTTGTAGCCTGTGGGCTCCTGCT*TCTCCTCCAGCATGTGCA*CGGTGAGACTGT	**WT**
	ATGCCT*TTGGCTAGACTTCCTGGT*TGGCTGTATGTTGTAGCCTGTGGGCTCCTGCT*TCTCCTCCAGCATGT* 49bp insertion *GCA*CGGTGAGACTGT	**△49bp**
4#	ATGCCT*TTGGCTAGACTTCCTGGT*TGGCTGTATGTTGTAGCCTGTGGGCTCCTGCT*TCTCCTCCAGCATGTGCA*CGGTGAGACTGT	**WT**
	ATGCCT*TTGGCTAGACTTCCT*.....*TGCA*CGGTGAGACTGT	**△49bp**
18#	ATGCCT*TTGGCTAGACTTCCTGGT*TGGCTGTATGTTGTAGCCTGTGGGCTCCTGCT*TCTCCTCCAGCATGTGCA*CGGTGAGACTGT	**WT**
	ATGCCT*TTGGCTAGACTTCC*.....*TGCA*CGGTGAGACTGT	**△50bp**
23#	ATGCCT*TTGGCTAGACTTCCTGGT*TGGCTGTATGTTGTAGCCTGTGGGCTCCTGCT*TCTCCTCCAGCATGTGCA*CGGTGAGACTGT	**WT**
	ATGCCT*T*.....TGT	**△76bp**
26#	ATGCCT*TTGGCTAGACTTCCTGGT*TGGCTGTATGTTGTAGCCTGTGGGCTCCTGCT*TCTCCTCCAGCATGTGCA*CGGTGAGACTGT	**WT**
	ATGCCT*TTGGCT*.....AGACTGT	**△67bp**

Fig.1

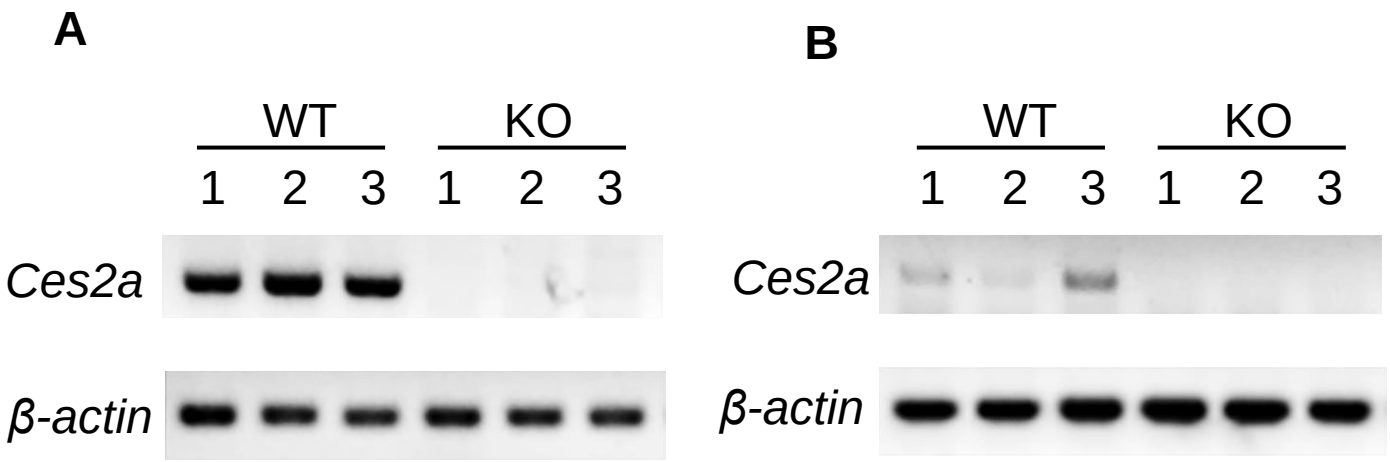

Fig.2

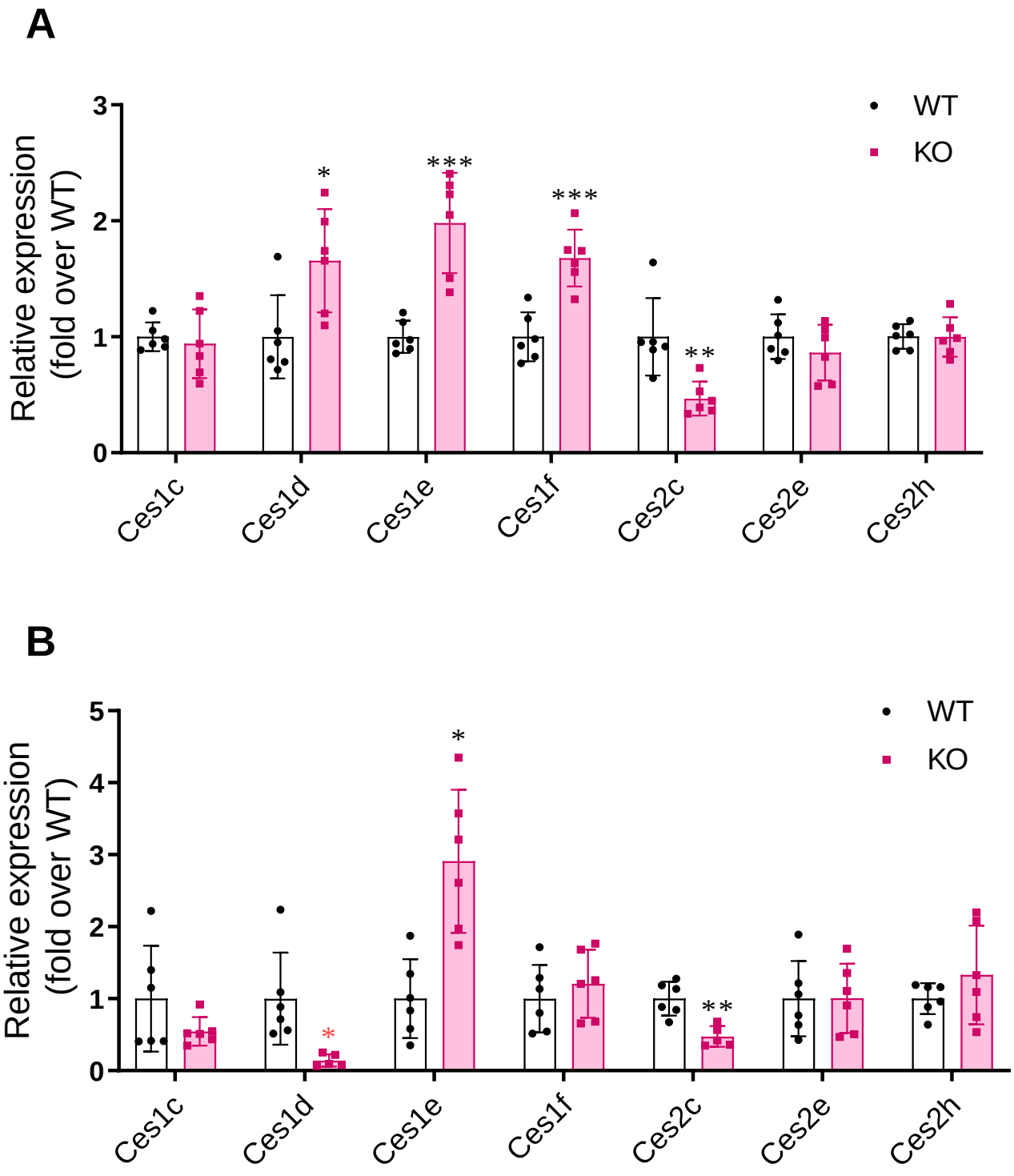
A
Relative expression
(fold over WT)
3
2
1
0
WT
KO
*
***
***
**
Ces1c
Ces1d
Ces1e
Ces1f
Ces2c
Ces2e
Ces2h
B
Relative expression
(fold over WT)
5
4
3
2
1
0
WT
KO
*
*
**
Ces1c
Ces1d
Ces1e
Ces1f
Ces2c
Ces2e
Ces2h

Fig.3

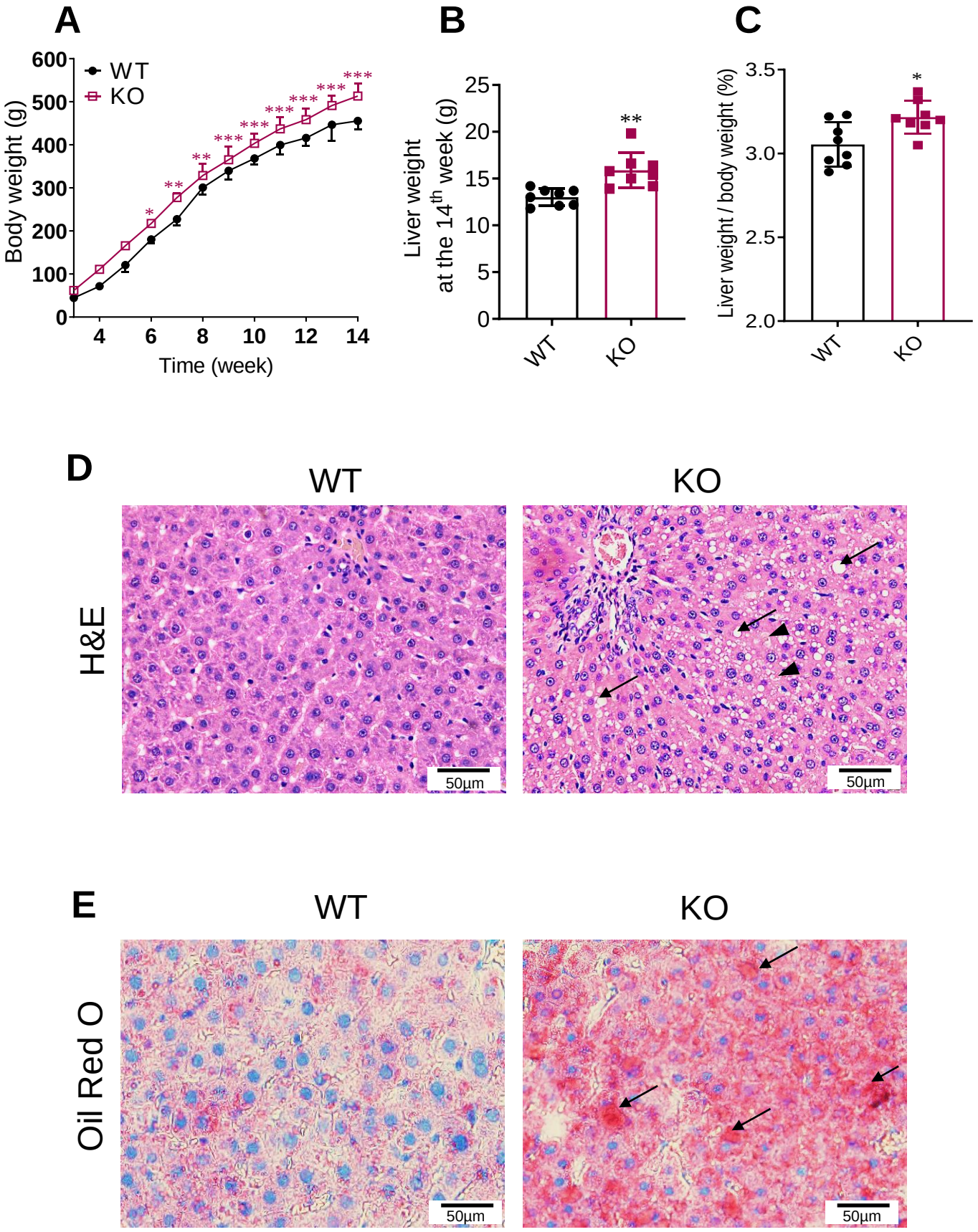
A
B
C
Body weight (g)
WT
KO
Time (week)
Liver weight at the 14th week (g)
Liver weight / body weight (%)
D
H&E
WT
KO
50μm
E
Oil Red O
WT
KO
50μm

Fig.4

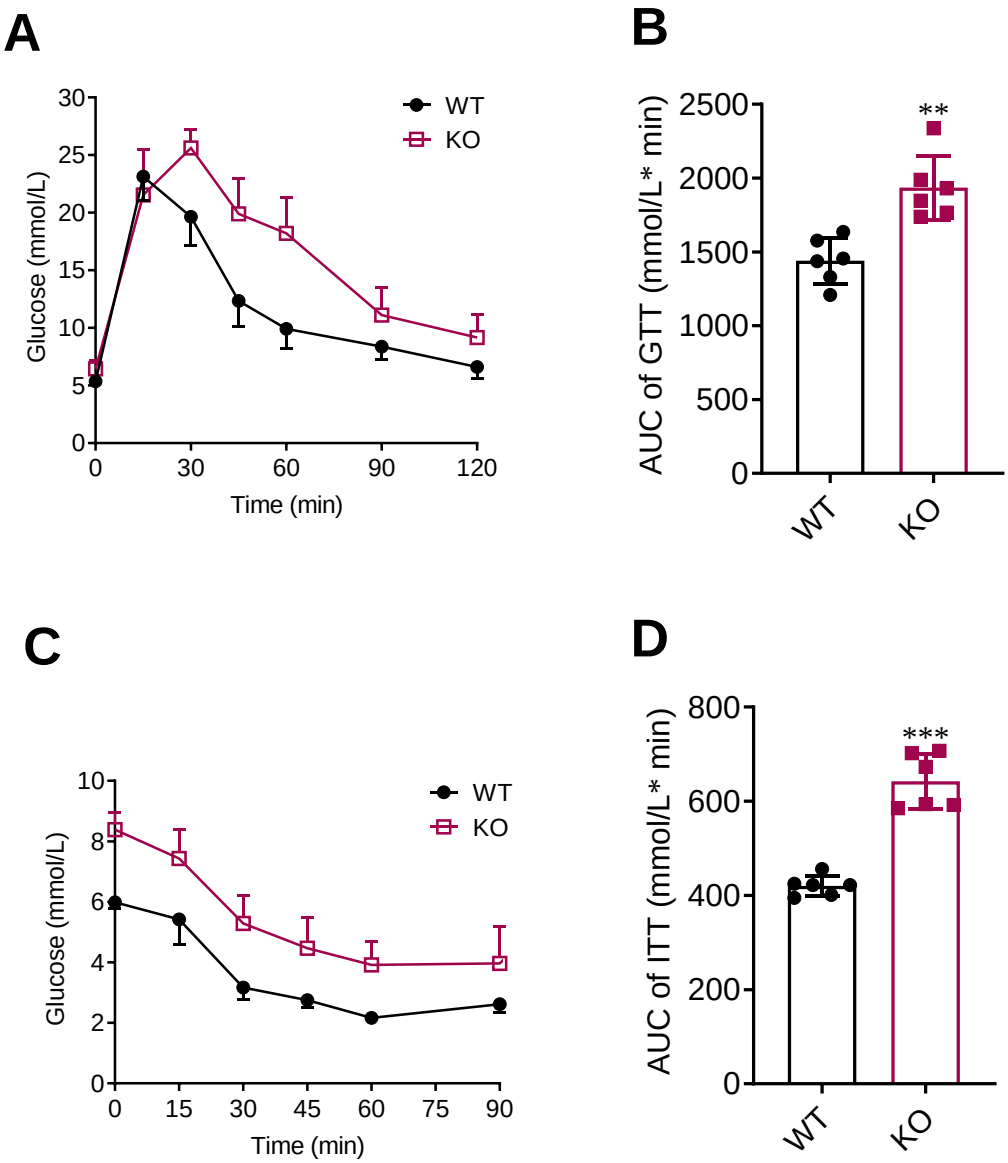
A
B
C
D
WT
KO
Glucose (mmol/L)
Time (min)
AUC of GTT (mmol/L* min)
AUC of ITT (mmol/L* min)
**
***

Fig.5

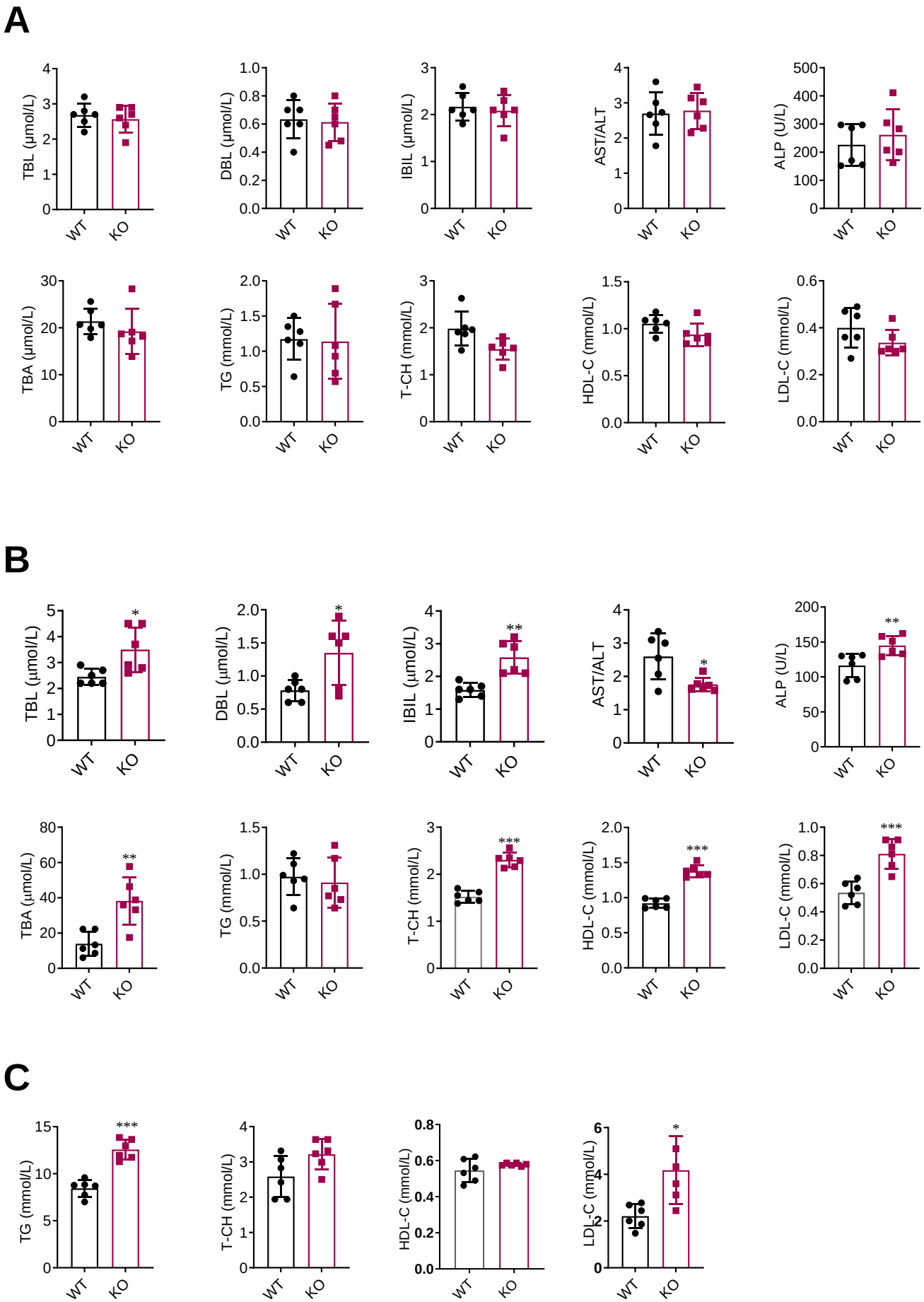
A
TBL (μmol/L)
DBL (μmol/L)
IBIL (μmol/L)
AST/ALT
ALP (U/L)
TBA (μmol/L)
TG (mmol/L)
T-CH (mmol/L)
HDL-C (mmol/L)
LDL-C (mmol/L)
WT
KO
B
TBL (μmol/L)
DBL (μmol/L)
IBIL (μmol/L)
AST/ALT
ALP (U/L)
TBA (μmol/L)
TG (mmol/L)
T-CH (mmol/L)
HDL-C (mmol/L)
LDL-C (mmol/L)
C
TG (mmol/L)
T-CH (mmol/L)
HDL-C (mmol/L)
LDL-C (mmol/L)

Fig.6

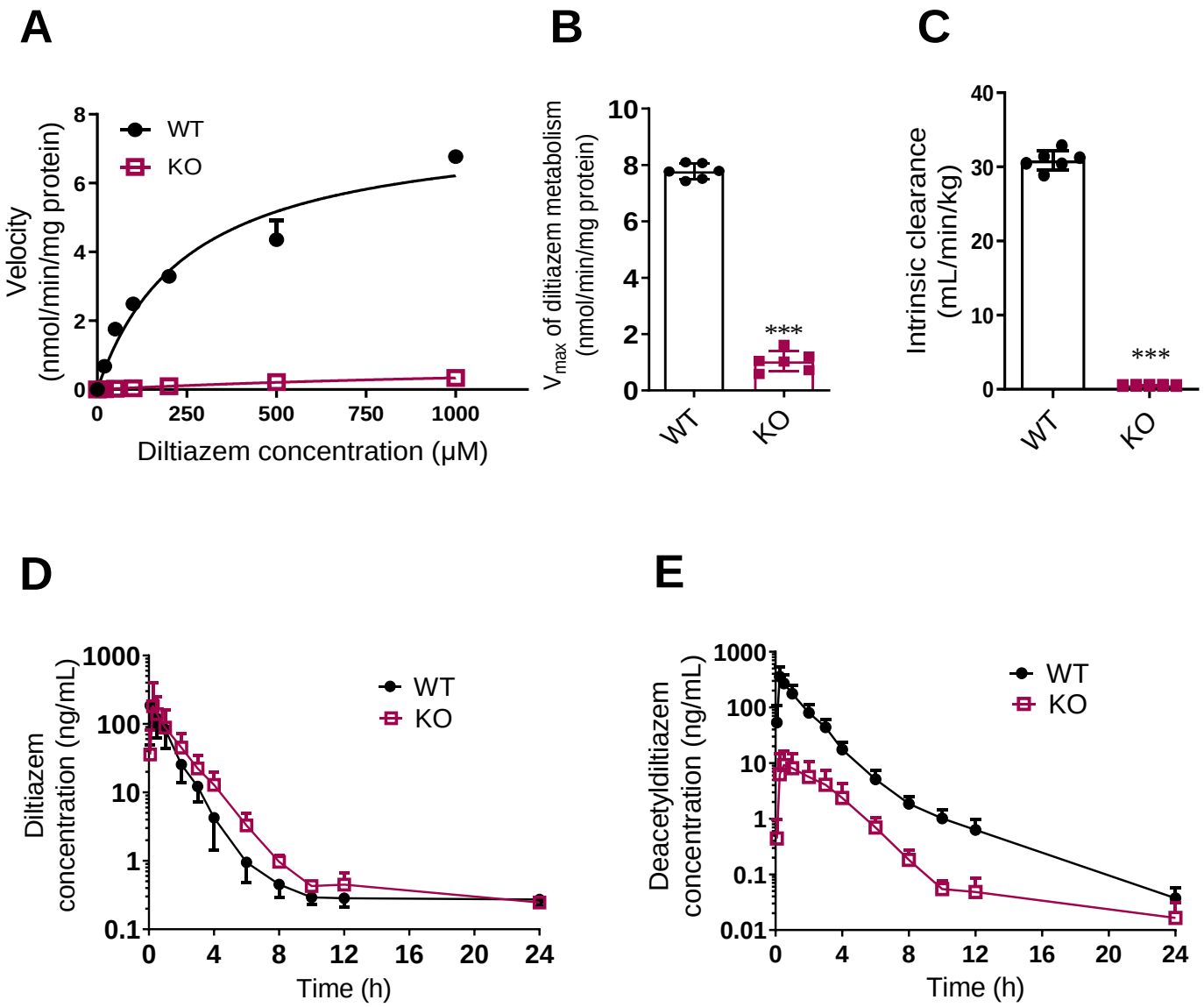
A
B
C
D
E
WT
KO
Velocity (nmol/min/mg protein)
Diltiazem concentration (μM)
V_{max} of diltiazem metabolism (nmol/min/mg protein)
Intrinsic clearance (mL/min/kg)
***
Diltiazem concentration (ng/mL)
Deacetyldiltiazem concentration (ng/mL)
Time (h)

Fig.7